International Research Journal of Engineering and Technology (IRJET) e-ISSN: 2395-0056
Volume: 07 Issue: 06 | June 2020 www.irjet.net p-ISSN: 2395-0072

B-lines Detection In-Vivo Lung using Morphological Image Processing

Mohammad Ashfaq[1], P. Varsha Ramya Sri[2], K. Bala Vara Prasad[3], N.Nagaraju[4]

[1, 2, 3] UG Student, Dept. of Electronics and Communication Engineering, Dhanekula Institute of Engineering and Technology, Vijayawada, Andhra Pradesh, India
[4] Assistant Professor, Dept. of Electronics and Communication Engineering, Dhanekula Institute of Engineering and Technology, Vijayawada, Andhra Pradesh, India

---

Abstract - *The main objective of this paper is accurate detection and visualization of B-lines in ultrasound lung images. Patterns of disease distribution within the secondary lobule have been well established pathologically. Identifying normal and abnormal components of the lobule is therefore a potential aid in distinguishing different parenchyma diseases. This designed feature is able to differentiate between the healthy and unhealthy classes based on B-lines in ultrasound lung images. B-lines are important ultrasound artifacts used in LUS for detection of pulmonary disease.*

Key Words: Ultrasound, image processing, pulmonary diseases, B-lines, pulmonary edema.

1. INTRODUCTION

Lung ultrasound (LUS) has received increasing attention in recent years, as it enables a quick visual evaluation of the lung tissue and pleura without imposing radiation [1]. B-lines are important ultrasound artifacts used in LUS for detection of pulmonary disease. They are defined as discrete laser-like vertical hyper echoic reverberation artifacts that arise from the pleura, spread down without fading to the edge of the screen, and move synchronously with lung sliding [2]. An intimate mixture of air and water characterizes the lung state. Change in their balance can be a sign of pulmonary disease. Interactions of water and air in ultrasound lung scans generate a variety of artifacts, and a LUS image of pulmonary disease is therefore based on analyzing these artifacts during visualization of the structures [3], [4], [5], [6]. B-lines are reverberation artifacts generated by multiple reflections of the ultrasound beam trapped between air- and water-rich structures.

They originate from the visceral pleura (serous membrane covering the surface of the lungs) and spread down to the edge of the screen. B-line detection is essential in the assessment of lung-edema in LUS imaging, which is often present in patients with heart and lung diseases as well as patients having undergone major surgery [5], [7], [8]. B-lines are also seen in patients with interstitial lung diseases and have been used to grade disease severity [9]. In daily clinical practice, patients suspected for pulmonary edema are imaged with X-ray, and often repeatedly imaged with short intervals to monitor the effect of the applied treatment. Lung ultrasound is a well-established modality, but it is often bypassed, as the medical staff handling these patients are not familiar with the method.

In 1997, Lichtenstein [10] showed a correlation between Blines in ultrasound, and chest computed tomography (CT) with edema. Even though LUS already had been used for evaluation of pleural effusion, it was the first time that the diagnostic value of B-line artifacts was shown. In 2004, Picano [11] showed the correlation between the number of B-lines detected by LUS and X-ray findings for assessing the presence of extra-vascular lung water (EVLW). Since then, multiple studies have shown the methodological validation and clinical application of Blines for diagnosing pulmonary diseases. The common practice for diagnosing pulmonary edema with ultrasound is based on visual analysis and interpretation of B-lines [4], [5], [6], [12].

Several B-lines distributed bilaterally in more scans on each lung defines diffuse alveolar-interstitial syndrome (caused by hydrostatic pulmonary edema, lesional pulmonary edema or fibrosis) [5]. The standard pathological routine for diagnosing this disease is to investigate the number of B-lines in a single scan or frame. A study performed by intensivists showed that the mean distance between two adjacent B-lines at the lung surface is never more than 7 mm, and this should be the widest distance between B-lines to be significant [3]. Another study used the criteria of counting at least three artifacts with a distance between adjacent lines of no more than 7 mm for identifying edema [13]. On the other hand, visualization of isolated B-lines, or visualization of multiple B-lines of more than 7 mm apart in a single scan, was considered a normal finding [13]. Major factors affecting the accuracy of the examination are interpretation error due to inexperience and habituation. Computer-assisted interpretation can potentially address the issue of these errors, and facilitate the adoption by users. A large multicenter study (n=1005) examined with six-zone scanning protocol the presence of B-lines. The LUS approach had a significantly higher accuracy in differentiating acute decompensated heart failure from noncardiac causes of acute dypnea when compared with clinical evaluation and chest radiography [14]. Another

large prospective study (n=788) was conducted for point-of-care ultrasonography [15]. Using LUS, improved diagnosing and faster treatment were given to the patients group treated with point-of-care ultrasonography compared with the control group. A systematic review study was conducted in 2014, with primary objective of determining the sensitivity and specificity of ultrasound using B-lines in diagnosing acute cardiogenic pulmonary edema (ACPE) in patients presenting to the emergency department with acute dyspnea [16]. The results showed that sensitivity of US using B-lines to diagnosis ACPE is 94.1% and the specificity is 92.4%. The results showed the importance of point-of-care lung ultrasound has shown promise as a diagnostic tool in this setting.

Apart from the recent advances in application of lung ultrasound, very few automated techniques for characterizing the B-line artifacts and pulmonary disease is presented in the literature. In 2013 a technique for B-line scoring was presented [17]. The technique used a polar reformatting technique to convert the images to a 60_40 rectangular grid, and extracted 5 features from each column to detect the B-lines. Moshavegh [18] presented an automated technique for detecting and characterizing B-lines. The technique first delineated the pleura on the scan using graphs, and then detected and visualized the B-lines on the B-mode. A computer-aided quantitative method for detection of pulmonary edema in mechanically ventilated cardiac surgery patients was presented in 2016 [19]. The technique analyzed the mean and standard deviation of grayscale changes in B-mode images to identify edema. Another study used Hough transform for detecting Blines [20]. The study compared the Hough transform algorithm with other automated techniques, as well as the previously presented technique by authors of this paper in [18].

The main purpose of this paper is to propose a method for accurate detection and visualization of B-lines in ultrasound lung scans, which provides a measure for the number of B-lines present. Section II introduces the proposed algorithm. Section III presents the ultrasound images, parameters to check quality of this study. Section IV presents the preliminary in-vivo results and discussion, and section V concludes the paper.

2. PROPOSED SYSTEM

Morphological filters by reconstruction with Semi Translation Invariant Contour-let transform that satisfy the above requirement of preserving edge information and introducing no fake contours. Opening by reconstruction will reconstruct edge information of the features, leading to the spread of edge and part of the foreground image information for improvement of PSNR of an image. Mean square error values of an image will be decreased after applying this STICT operation.

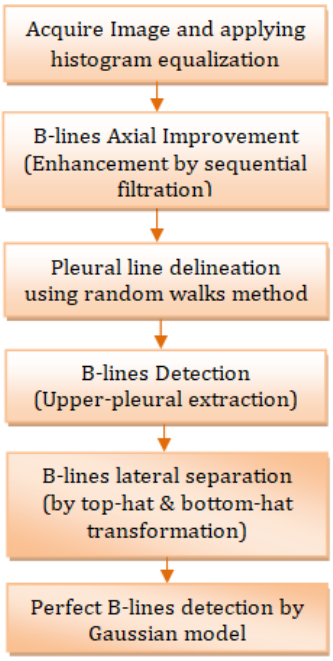

Fig-1: Block diagram

2.1 ACQUIRING THE IMAGE

The image which we use is the sonographic image of the lungs. This image is used as an input to the next coming processes. To this image histogram equalization is done so that to spread the pixels across the image effectively.

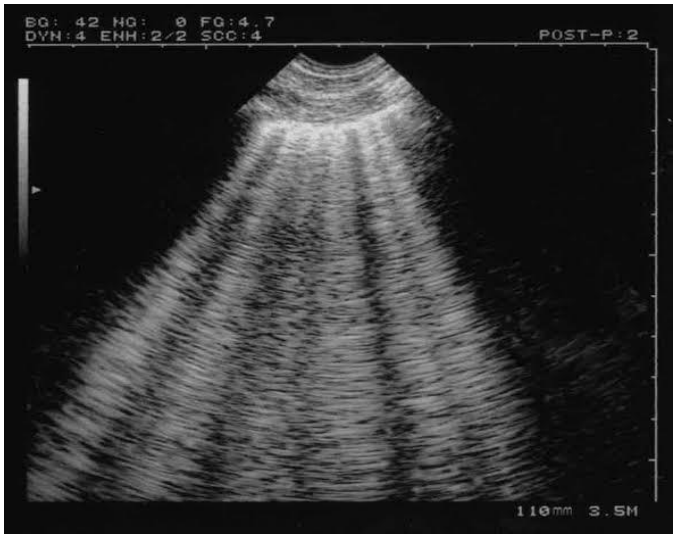

Fig-2: Ultrasound Image of A-lines & B-lines

2.2 PLEURAL LINE DELINEATION

This method is used for locating the exact pleural line on the lung scans. This method measures the uncertainty in attenuated and/or shadow regions, and generates a normalized gray scale map. Properties of ultrasound are the attenuation of the signal by increasing depth. Beer–

Lambert Law was used to express the depth dependent attenuation, attenuated signal.

$$I=Io \exp(-\alpha d)$$

Io=initial intensity, α =attenuation co-efficient, d=distance from the source ultrasound lung images depict a clear distinction along the pleural line due to the abrupt change in the attenuation.

2.3 B-LINE DETECTION

The obtained output of the image after pleural line delineation the area of the image is kept to scan and exclude the corresponding upper-pleura (because B-lines originate from the pleura and extend downwards to the end of the) screen. Using a normalized cumulative histogram the remained RF data will be computed axially. Each column of the axial-cumulative image will be normalized to the maximum brightness of the same column. This image will be inverted, and adaptive histogram equalization was performed to increase the contrast binary mask including regions with gray scale values higher than 0.5 inside the histogram-equalized image will be generated. Hilbert transformation, to compute envelope of RF data. Compute discrete gray scale image. Axial cumulative sum and normalizing to the maximum intensity of that column.

$$Ax\_cdf(i,ii) = \frac{\sum_{j=0}^{i} Env(j,ii)}{\max(Env(ii).col)}$$

Inverting the axial cumulative image and perform adaptive histogram equalization

$$Bc = \max(Ax\_cdf) - Ax\_cdf$$
$$Bc = adapthisteq(Bc)$$

2.4 B-LINES LATERAL SEPARATION

Above yielded output consists axially elongated and adjacent tails. To separate and extract the B-lines automatically, a top-hat transformation will be used. Top-hat transform will be applied using a line structuring element (B) that was longer than the size of the connected regions.

The generated mask in the previous step contains prominent axially elongated and adjacent tails, which locate the B-lines. However, the tails can be laterally connected, which deteriorates the clean separation of B-lines. To separate and extract the B-lines automatically, a top-hat transformation was used. The top-hat transformation originally proposed by Mayer [24] is a mathematical morphology operator that uses morphological opening or closing for extracting bright (respectively dark) objects from an uneven background in a 2D grey-scale image. Top-hat transformation can be formulated in two ways: white top-hat (WTH) and black top-hat (BTH). WTH can also be used to identify prominent peaks in a 1D signal, and the BTH as the dual of the WTH can be used to identify the prominent minima in a 1D signal. In this study, a (WTH) with a flat disk structuring element was used to extract the B-lines.

2.5 B-LINE AXIAL IMPROVEMENT

An alternate sequential filtering (ASF) procedure using a repeated sequential morphological opening and closing will be applied to the mask. ASF highlights the vertical B-lines and isolate them from each other laterally. An axial line-structuring element along the ultrasound beam, was used for ASF filtering.

ASF closes small gaps axially and isolates the objects laterally. This was used to ensure that only elongated and axial information (B-line artifacts) in the compressed data is preserved and highlighted.

2.6 TOP –HAT TRANSFORMATION

Morphological filters by reconstruction that satisfies the above requirement of preserving edge information and introducing no fake contours. Opening by reconstruction will reconstruct edge information of the features. Opening by reconstruction will reconstruct edge information of the features, leading to the spread of edge and part of the foreground image information being removed.

$$T_t(f) = f - f \circ b$$

2.7 BOTTOM-HAT TRANSFORMATION

Dual the bottom-hat transform, is defined as the residual of a closing compared to the original signal. Therefore, one can use hat-transforms with increasing size of the structuring element to extract details of increasing size. By performing repeated hat-transforms with increasing size of the structuring element on the signal, we can build the morphological hat scale spa. Bottom hat transforms are used to obtain the bottom scale space, in which all valleys of the signal are desired

$$Tb(f) = f \bullet b - f$$

Both top-hat transforms are images that contain only non-negative values at all pixels.

2.8 GAUSSIAN MODEL FITTING

Above yielded output is quite rough, the peak points of the B-lines were not well-defined. Gaussian model fitting is used to represent them.

$$y = Ae^{-(x-\mu)^2/2\alpha^2}$$

A =height of the peak and
μ= controlling its width
y= amplitude range of the observed data points.

3. ULTRA SOUND IMAGES

Ultrasound scans are used to evaluate fetal development, and they can detect problems in the liver, heart, kidney, or abdomen. They may also assist in performing certain types of biopsy. The image produced is called a sonogram.

The risk of pulmonary edema is the main limiting factor in fluid therapy in the critically ill. Interstitial edema is a subclinical step that precedes alveolar edema. This study assesses a bedside tool for detecting interstitial edema, lung ultrasound. The A-line is a horizontal artifact indicating a normal lung surface. The B-line is a kind of comet-tail artifact indicating subpleural interstitial edema.

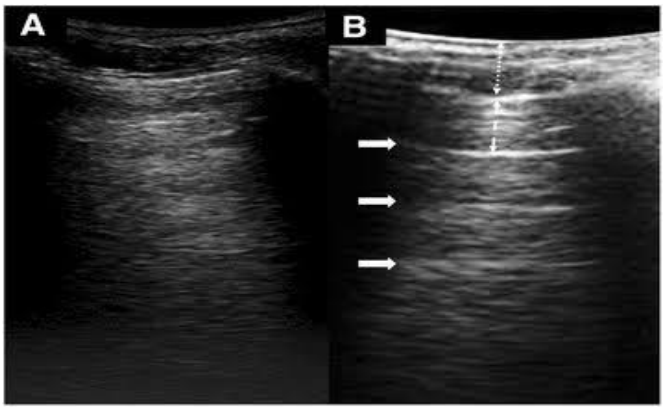

Fig-3: Images of A-lines & B-lines

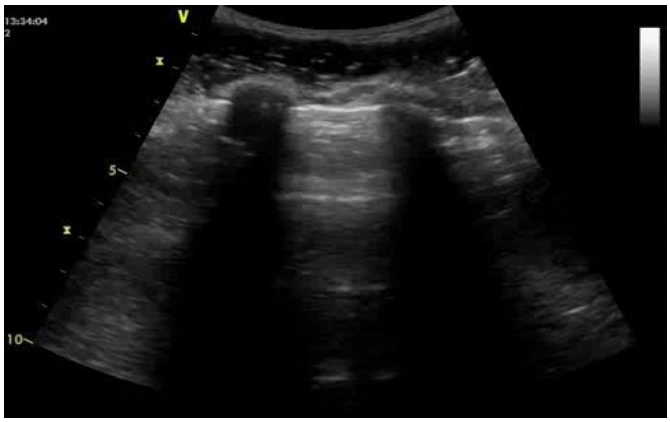

Fig-4: Ultrasound image of lungs

3.1 PARAMETERS TO CHECK THE QUALITY OF THE IMAGE

After all the processing is done it essential to check the quality of the image. Quality can we reduced mostly due to the noise present in the Ultrasound image. Here we considered Peak Signal-to-noise ratio (PSNR) and Mean-square error to be the parameters that help to decide or check the quality of the image.

$$PSNR = 10\log_{10}\left(\frac{MAX_I^2}{MSE}\right)$$

$$PSNR = 20\log_{10}\left(\frac{MAX_I}{\sqrt{MSE}}\right)$$

$$PSNR = 20\log_{10}(MAX_I) - 10\log_{10}(MSE)$$

$$MSE = \frac{1}{mn}\sum_{i=0}^{m-1}\sum_{j=0}^{n-1}[I(i,j) - K(i,j)]^2$$

4. RESULTS & DISCUSSION

After all the step by step processing done to the image now we can say that the detection of B-lines in an ultrasound image of the lungs is accurate and efficient. The PSNR value obtained in the recent processing is 98.0328 with an MSE of 1.9672.

The following are the images of ultrasound after processing.

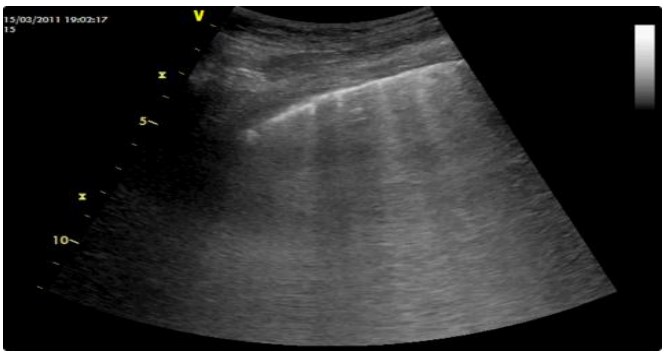

Fig-5: Lung Ultrasound given as input to MATLAB for processing

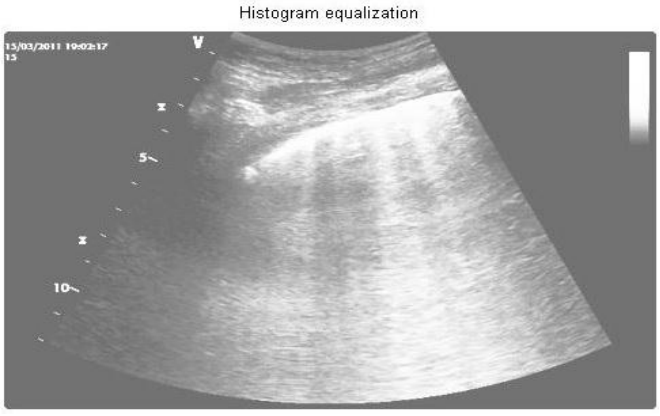

Fig-6: Histogram equalization of original image

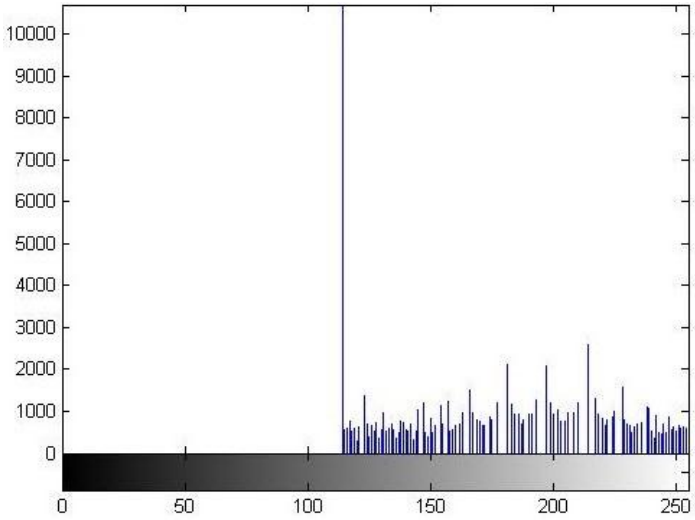

Fig-7: Distribution of pixels after histogram equalization

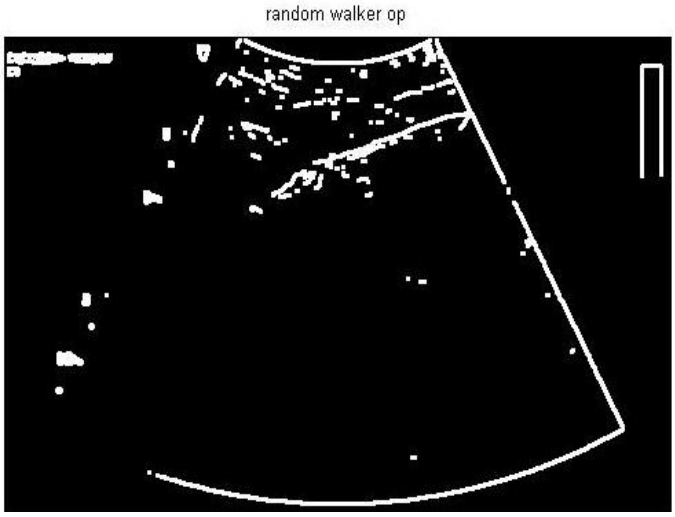

Fig-10: Image after applying Random walk method

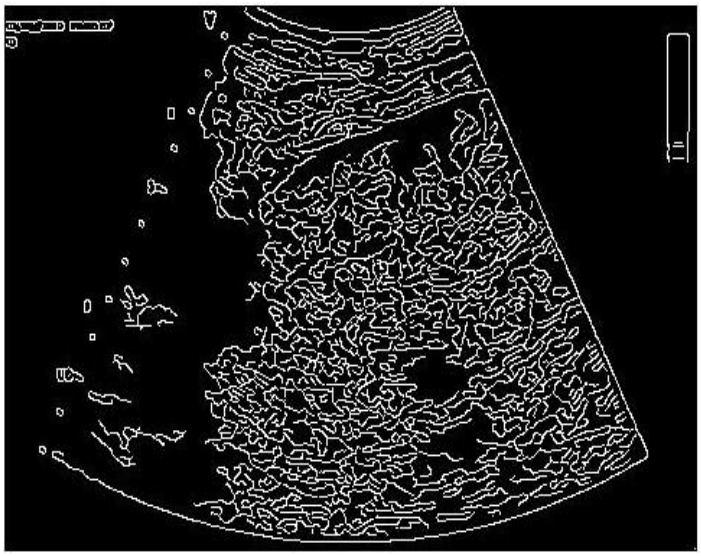

Fig-8: Image after Edge detection

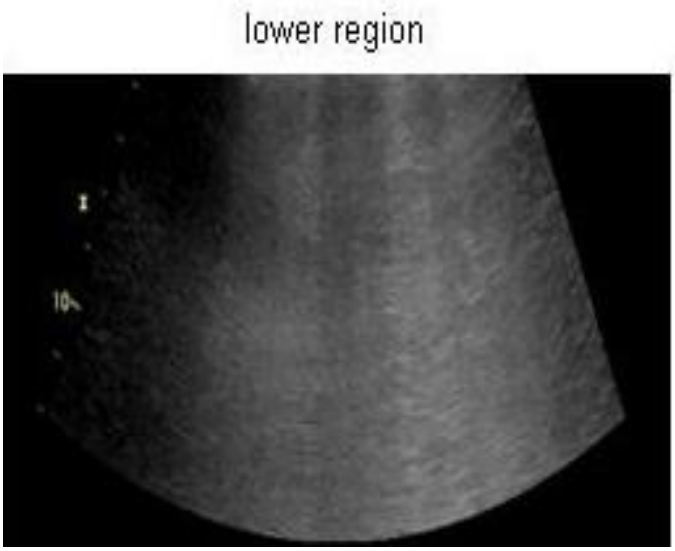

Fig-11: Image after clearing the upper-pleural section ultrasound image

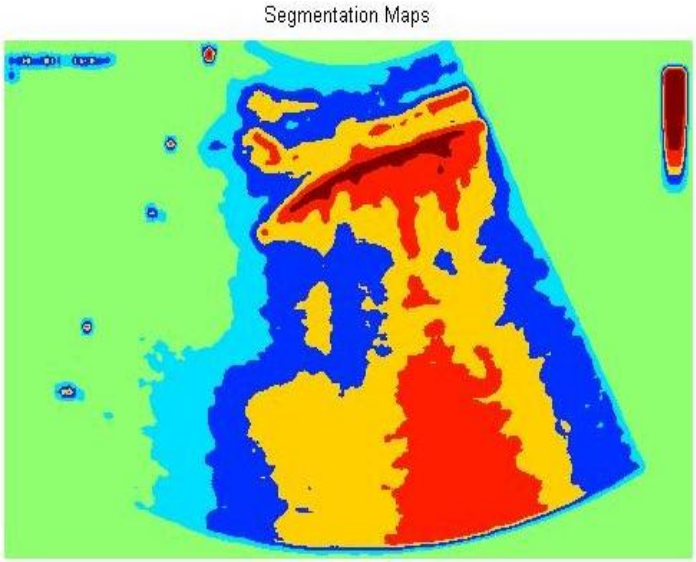

Fig-9: Image showing segmentations

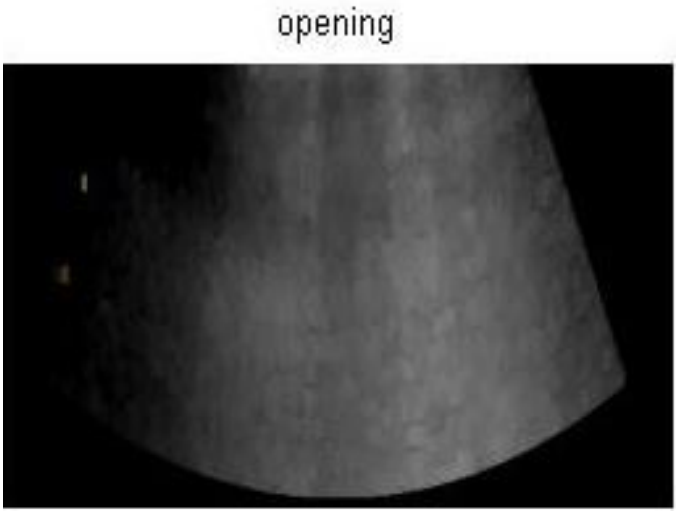

Fig-12: Opening performed to the image

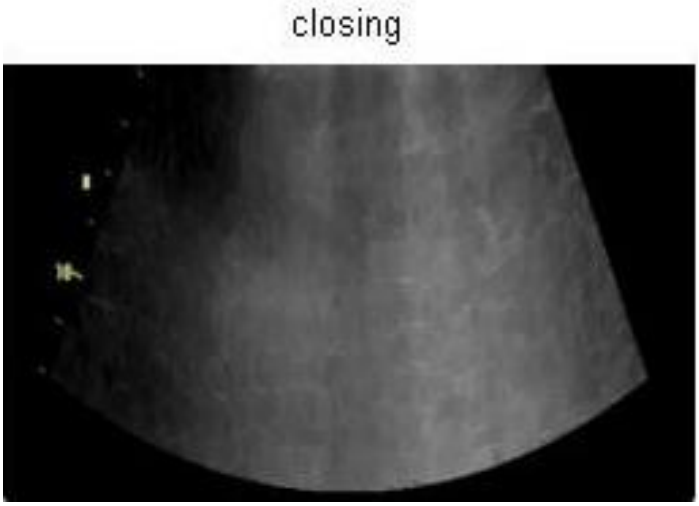

Fig-13: Image after closing

Fig-15: Image after Bottom-hat transformation

Fig-14(a)

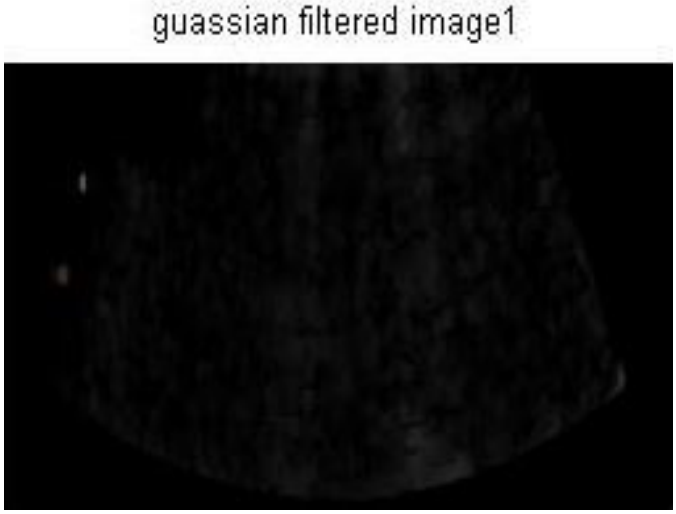

Fig-16(a)

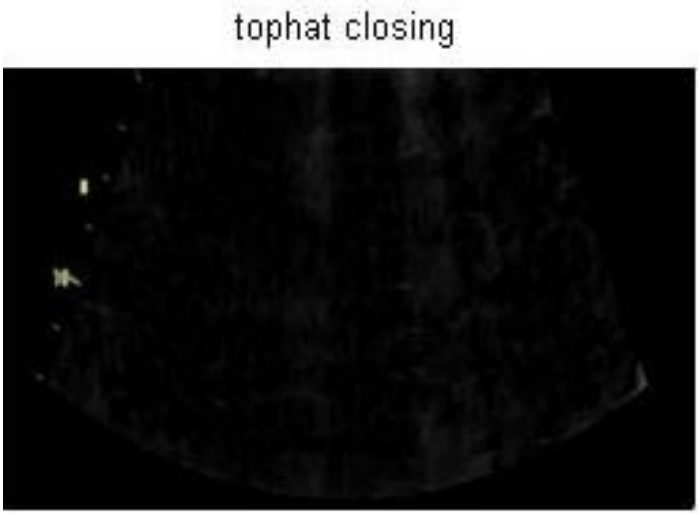

Fig-14(b)

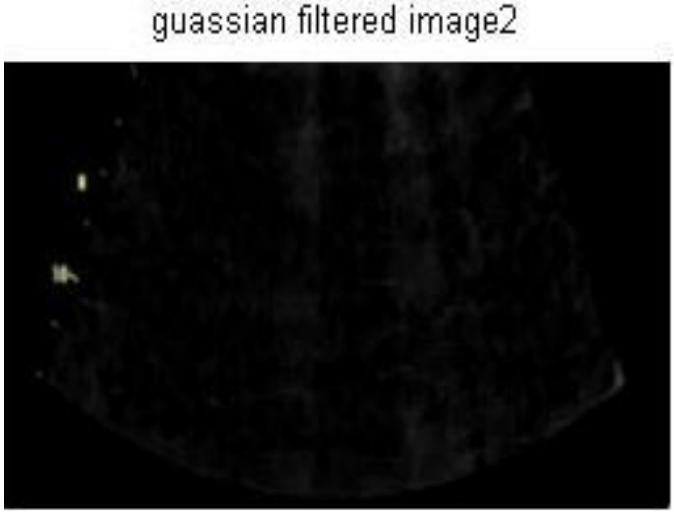

Fig-16(b)

Fig-14: (a, b) Images after applying top-hat transformation

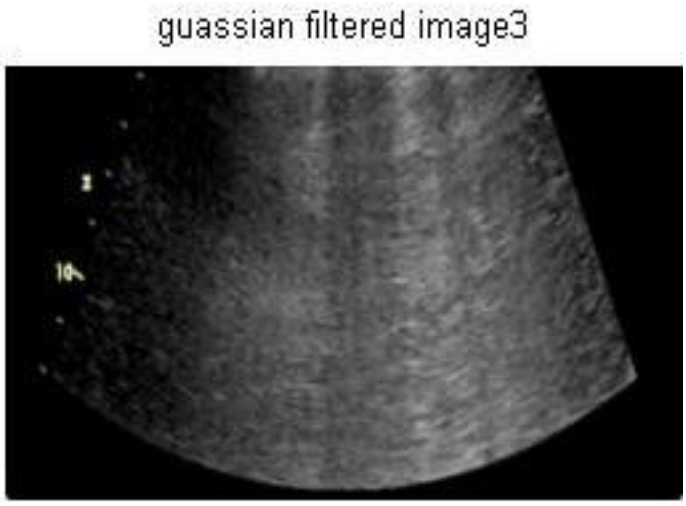

Fig-16(c)

Fig-16: (a, b, c) Images after gaussian model fitting

Fig-17: Dialogue box stating B-lines existing in the image provided as input

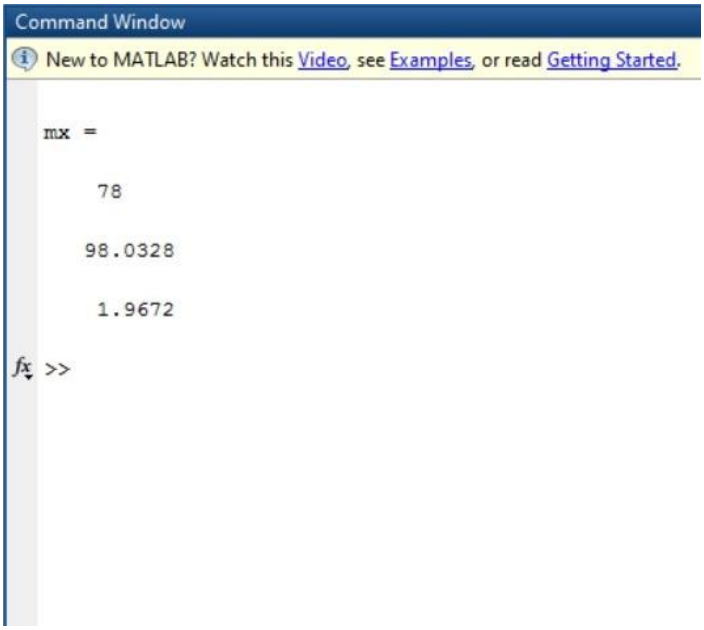

Fig-18: PSNR & MSE values of the output obtained

5. CONCLUSION

Patterns of disease distribution within the secondary lobule have been well established pathologically. Normal and abnormal components of the lobule are observed and pulmonary lung diseases can be identified. These lung diseases can be also be the side effects of the problems generated in the heart and preventive measures can be taken at early stages.

REFERENCES

[1] C. F. Dietrich, G.Mathis, M. Blaivas, G. Volpicelli, A. Seibel, D. Wastl, N. S. S. Atkinson, X. W. Cui, M. Fan, and D. Yi, "Lung b-line artefacts and their use," Journal of Thoracic Disease, vol. 8, no. 6, pp. 1356–1365, 2016.

[2] G. Volpicelli, M. Elbarbary, M. Blaivas, D. L. A., G. Mathis, A. W. Kirkpatrick, L. Melniker, L. Gargani, V. E. Noble, G. Via, A. Dean, and J. W. Tsung, "International evidence-based recommendations for point-of-care lung ultrasound," Intensive Care Medicine, vol. 38, no. 4, pp. 577–591, 2012.

[3] D. Lichtenstein, G. Meziere, P. Biderman, and A. Gepner, "The comettail artifact: An ultrasound sign ruling out pneumothorax," Intensive Care Med., vol. 25, no. 4, pp. 383–388, 1999.

[4] E. Agricola, T. Bove, M. Oppizzi, G. Marino, A. Zangrillo, A. Margonato, and E. Picano, "Ultrasound comet-tail images: A marker of pulmonary edema: A comparative study with wedge pressure and extravascular lung water," Chest, vol. 127, no. 5, pp. 1690–1695, 2005.

[5] G. Volpicelli, A. Mussa, G. Garofalo, L. Cardinale, G. Casoli, F. Perotto, C. Fava, and M. Frascisco, "Bedside lung ultrasound in the assessment of alveolar-interstitial syndrome," Am. J. Emerg. Med., vol. 24, no. 6, pp. 689–696, 2006.

[6] L. Gargani, F. Frassi, G. Soldati, P. Tesorio, M. Gheorghiade, and E. Picano, "Ultrasound lung comets for the differential diagnosis of acute cardiogenic dyspnoea: A comparison with natriuretic peptides," Eur. J. Heart Failure, vol. 10, no. 1, pp. 70–77, 2008.

[7] L. Gargani, "Lung ultrasound: A new tool for the cardiologist," Cardiovascular ultrasound, vol. 9, no. 1, 2011.

[8] D. A. Lichtenstein, "Lung ultrasound in the critically ill," Ann Intensive Care, vol. 4, no. 1, 2014.

[9] A. Hasan and H. Makhlouf, "B-lines: Transthoracic chest ultrasound signs useful in assessment of interstitial lung diseases," Annals of Thoracic Medicine, vol. 9, no. 2, pp. 99–103, 2014.

[10] D. Lichtenstein, G. M´ezi`ere, P. Biderman, A. Gepner, and O. Barr´e, "The comet-tail artifact. an ultrasound sign of alveolar-interstitial syndrome," Am. J. Respir. Crit. Care. Med., vol. 156, no. 5, pp. 1640–1646, 1997.

[11] Z. Jambrik, S. Monti, V. Coppola, E. Agricola, G. Mottola, M. Miniati, and E. Picano, "Usefulness of ultrasound lung comets as a nonradiologic sign of extravascular lung water," Am. J. Cardiology, vol. 93, no. 10, pp. 1265–1270, 2004.

[12] L. Gargani, V. Lionetti, C. D. Cristofano, G. Bevilacqua, F. Recchia, and E. Picano, "Early detection of acute lung injury uncoupled to hypoxemia in pigs using

ultrasound lung comets," Crit Care Med., vol. 35, no. 12, pp. 2769–2774, 2007.

[13] G. Volpicelli, L. Cardinale, G. Garofalo, and A. Veltri, "Usefulness of lung ultrasound in the bedside distinction between pulmonary edema and exacerbation of COPD," Am. Soc. Emerg. Radiol., vol. 15, no. 3, pp. 145–151, 2008.

[14] E. Pivetta, A. Goffi, E. Lupia, M. Tizzani, G. Porrino, E. Ferreri, G. Volpicelli, P. Balzaretti, A. Banderali, A. Iacobucci, S. Locatelli, and G. Casoli, "Lung ultrasound-implemented diagnosis of acute decompensated heart failure in the ed," Chest, vol. 148, no. 1, pp. 202– 210, 2015.

[15] C. B. Laursen, E. Sloth, A. T. Lassen, R. d. Christensen, J. Lambrechtsen, P. H. Madsen, D. P. Henriksen, J. R. Davidsen, and F. Rasmussen, "Pointof- care ultrasonography in patients admitted with respiratory symptoms: a single-blind, randomised controlled trial," The Lancet Respiratory Medicine, vol. 2, no. 8, pp. 638–646, 2014.

[16] M. A. Deeb, S. Barbic, R. Featherstone, J. Dankoff, and D. Barbic, "Point-of-care ultrasonography for the diagnosis of acute cardiogenic pulmonary edema in patients presenting with acute dyspnea: A systematic review and meta-analysis," Academic Emergency Medicine, vol. 21, no. 8, pp. 843–852, 2014.

[17] L. J. Brattain, B. A. Telfer, A. S. Liteplo, and V. E. Noble, "Automated B-line scoring on thoracic sonography," J. Ultrasound Med., vol. 32, no. 12, pp. 2185–2190, 2013.

[18] R. Moshavegh, K. L. Hansen, H. M. S. M. C. Hemmsen, C. E. andv M. B. Nielsen, and J. A. Jensen, "Novel automatic detection of pleura and B-lines (comet-tail artifacts) on in vivo lung ultrasound scans," in Proc. SPIE Med. Imag., vol. 9790, 2016, pp. 97 900K–97 900K–7.

[19] F. Corradi, C. Brusasco, A. Vezzani, G. Santori, T. Manca, L. Ball, F. Nicolini, T. Gherli, and V. Brusasco, "Computer-aided quantitative ultrasonography for detection of pulmonary edema in mechanically ventilated cardiac surgery patients," Chest, vol. 150, no. 3, pp. 640– 651, 2016.

[20] N. Anantrasirichai, W. Hayes, M. Allinovi, D. Bull, and A. Achim, "Line detection as an inverse problem: Application to lung ultrasound imaging," IEEE Trans. Med. Imag., vol. 36, no. 10, pp. 2045–2056, 2017.

[21] L. Grady, "Random walks for image segmentation," IEEE. Trans Patt. Ana. Mach. Int., vol. 28, no. 11, pp. 1768–1783, Nov 2006.

[22] A. Karamalis, W. Wein, T. Klein, and N. Navab, "Ultrasound confidence maps using random walks," Med. Image Anal., vol. 16, no. 6, pp. 1101– 1112, 2012.

[23] R. C. Gonzalez and R. E. Woods, Digital Image Processing, 3rd ed. Upper Saddle River, NJ, USA: Prentice-Hall, Inc., 2006.

[24] F. Meyer, "Contrast features extraction, special issues of practical metallography," in Quant. Anal. Microstruct. Mat. Sc. Bio. Med., vol. 8, 1977.

[25] S. Coiro, p. Rossignol, G. Ambrosio, E. Carluccio, G. Alunni, A. Murrone, I. Tritto, F. Zannad, and N. Girerd, "Prognostic value of residual pulmonary congestion at discharge assessed by lung ultrasound imaging in heart failure," European Journal of Heart Failure, vol. 17, no. 11, pp. 1172–1181, 2015.

[26] G. R. Bernard, A. Artigas, K. L. Brigham, J. Carlet, K. Falke, L. Hudson, M. Lamy, J. R. Legall, A. Morris, and R. Spragg, "The american-european consensus conference on ards. definitions, mechanisms, relevant outcomes, and clinical trial coordination." Am. J. Resp. Crit. Car. Med., vol. 149, no. 3, pp. 818–824, 1994.

[27] A. Fein, R. F. Grossman, J. G. Jones, E. Overland, L. Pitts, J. F. Murray, and N. C. Staub, "The value of edema fluid protein measurement in patients with pulmonary edema," Am. J. Med., vol. 67, no. 1, pp. 32–38, 1979.

[28] A. Kratz, M. Ferraro, P. M. Sluss, and K. B. Lewandrowski, "Case records of the massachusetts general hospital. weekly clinicopathological exercises. laboratory reference values." N. Engl. J. Med., vol. 351, no. 23, pp. 1548–1563, Oct 2004.

[29] Ramin Moshavegh, Kristoffer Lindskov Hansen, Hasse Moller Sorensen, Michael Bachmann Nielsen, and Jorgen Arendt Jensen "Automatic Detection of B-lines in In-Vivo Lung Ultrasound" IEEE Transactions on Ultrasonics, Ferroelectrics, and Frequency Control, vol. 66 issue: 2, 2019.